"Giant" Enhancement of the Upper Critical Field and Fluctuations above the Bulk T_c in Superconducting Ultrathin Lead Nanowire Arrays

Mingquan He,[†,§] Chi Ho Wong,[†,§] Pok Lam Tse,[†] Yuan Zheng,[†] Haijing Zhang,[†] Frank L. Y. Lam,[‡] Ping Sheng,[†] Xijun Hu,[‡] and Rolf Lortz[†,*]

[†]Department of Physics and the William Mong Institute of Nano Science and Technology, Hong Kong University of Science and Technology, Clear Water Bay, Kowloon, Hong Kong, People's Republic of China, and [‡]Department of Chemical and Biomolecular Engineering, Hong Kong University of Science and Technology, Clear Water Bay, Kowloon, Hong Kong, People's Republic of China. [§]M. He and C. H. Wong contributed equally to this work.

ABSTRACT We have produced ultrathin lead (Pb) nanowires in the 6 nm pores of SBA-15 mesoporous silica substrates by chemical vapor deposition. The nanowires form regular and dense arrays. We demonstrate that bulk Pb (a type-I superconductor below $T_c = 7.2$ K with a critical field of 800 Oe) can be tailored by nanostructuring to become a type-II superconductor with an upper critical field (H_{c2}) exceeding 15 T and signs of Cooper pairing 3−4 K above the bulk T_c. The material undergoes a crossover from a one-dimensional fluctuating superconducting state at high temperatures to three-dimensional long-range-ordered superconductivity in the low-temperature regime. We show with our data in an impressive way that superconductivity in elemental metals can be greatly enhanced by nanostructuring.

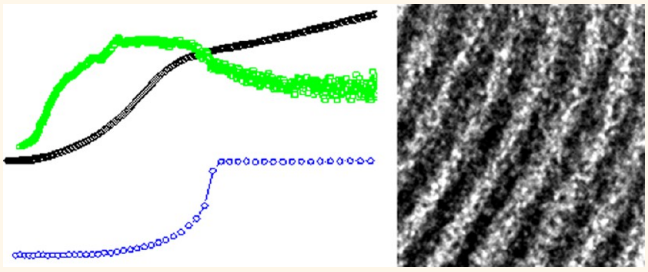

KEYWORDS: superconductivity · nanowires · mesoporous silica matrixes · thermodynamic properties · electric transport

The greatest opportunity that nanotechnology brings is the possibility to tailor materials through nanostructuring. The confined geometry can have various effects on superconducting materials; for example, a slight increase of the superconducting transition temperature was observed in nanoparticles of In,[1,2] Tl,[1] and Ga[3−5] and Pb nanobelts,[6,7] some enhancement of the critical fields,[2,4,6−9] and unusual magnetoresistance oscillations.[6,7] Quasi-one-dimensional (quasi-1D) behavior occurs in nanowires that are thinner than their superconducting coherence length.[10,11] In the extreme 1D limit of metallic nanowires, Van Hove singularities are formed in the electronic density of states.[12] According to the Bardeen−Cooper−Schrieffer (BCS) theory, a high density of states at the Fermi level is one of the most important ingredients for a superconductor with a high T_c. Quasi-1D superconductors thus have the potential for T_c's well above that of the material in its bulk form. Unfortunately, the Mermin, Wagner, and Hohenberg theorem[13,14] predicts that, in dimensions smaller than 3D, any long-range-ordered physical state will be suppressed at finite temperatures. In a quasi-1D superconducting material thermally induced phase slips in the order parameter will cause finite resistance at $T > 0$ K.[15,16] However, when many quasi-1D elements are parallel and form arrays, it was predicted from theory[17−24] and experimentally demonstrated[25,26] that a 3D long-range-ordered state can be formed, if these elements are weakly coupled in the lateral plane.

Bulk Pb is a well-known elementary superconductor with 83 nm coherence length. Therefore, Pb nanowires thinner than ~80 nm are potential candidates to study the complex quasi-1D superconducting transition and associated finite size effects. Pb nanowire arrays have been investigated previously, but only for diameters of 56 nm or above.[27] Our nanowires fabricated in the 6 nm pores of SBA-15 silica (Pb-SBA-15) are 1 order of magnitude thinner.

* Address correspondence to lortz@ust.hk.

Received for review February 4, 2013 and accepted April 4, 2013.

Published online April 08, 2013
10.1021/nn400604v

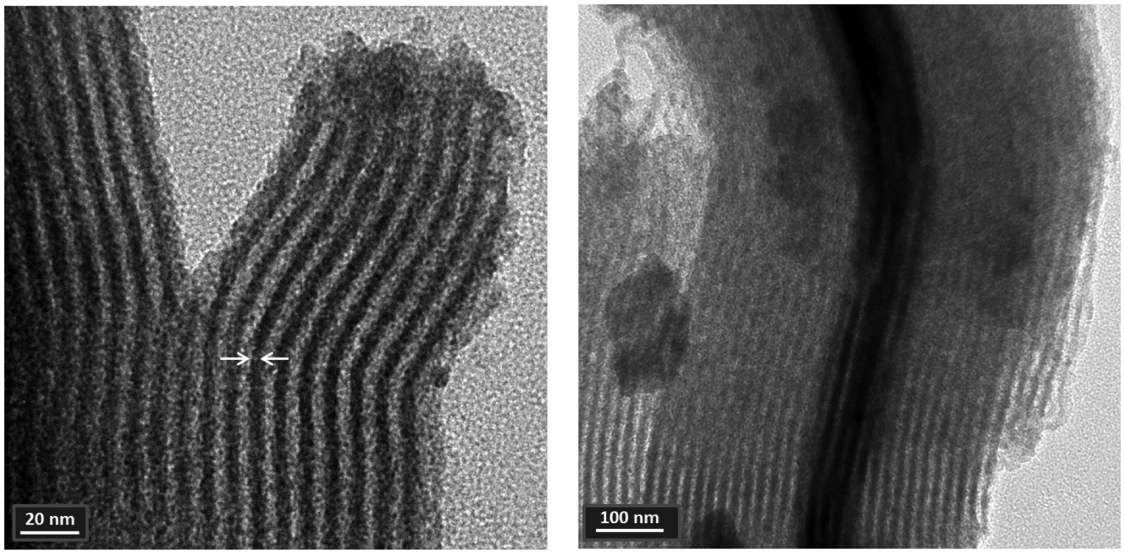

Figure 1. TEM images of the arrays of parallel Pb nanowires (dark gray, the white arrows mark the walls of one of them) in the 6 nm pore channels of SBA-15 mesoporous silica crystals (light gray).

A significant fraction of their atoms is located within the surface layer, which may have significant effects on their superconducting characteristics. This composite material is a powder of polycrystalline grains with diameters up to a few 100 μm. Figure 1 shows transmission electron microscopy (TEM) images of the encapsulated Pb nanowires. The parallel dark gray lines (indicated by the arrows) represent the nanowires within the SBA-15 host (light gray). The image shows a perfect filling factor of the pores in single crystals with diameters of a few 100 nm. The typical lengths of the SBA-15 single crystals range from 500 nm to several micrometers. The pores, in which the nanowires form regular and dense 3D arrays at a center-to-center distance of 9 nm, are occupied over their full length. According to our TEM images, the thickness of the nanowires can be estimated as ~5 nm. To examine their superconducting properties, we performed magnetization, specific-heat, and electrical transport measurements.

Magnetization. In Figure 2a the zero-field-cooled (ZFC) and field-cooled (FC) magnetization data of Pb-SBA-15 are plotted in comparison to normalized data of bulk Pb. A clear Meissner effect is observed for Pb-SBA-15. At first sight the superconducting transition remains in the vicinity of the bulk T_c at 7.2 K. The quasi-1D nature of the material causes obviously a more continuous transition in contrast to the sudden occurrence of the Meissner effect in bulk Pb. The magnetization reaches a temperature-independent value only below 3 K. The nanostructuring induces a certain flux pinning, recognizable in the form of a difference between the ZFC and FC branches. The presence of flux pinning and a Meissner effect below ~7 K means that macroscopic screening currents can be formed, which requires transverse tunneling currents between the

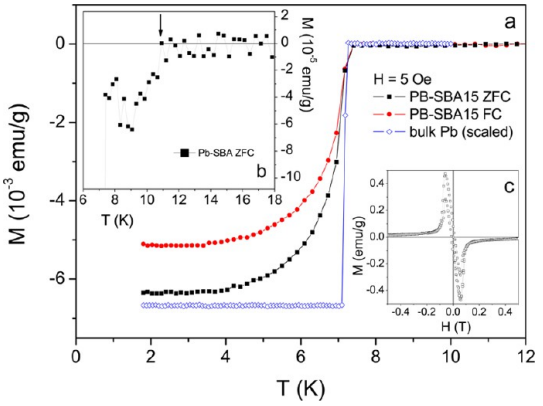

Figure 2. (a) Meissner signal in the magnetization of Pb-SBA-15. Filled squares represent ZFC data and open circles FC data compared to data of bulk Pb (stars). (For the latter, the data were scaled for comparison and the ZFC and FC curves were identical.) (b) Magnification of the onset of the superconducting transition of Pb-SBA-15 under ZFC conditions. A fairly sharp downturn shows the beginning of diamagnetic fluctuations at 11 K. (c) Field-sweep data for Pb-SBA-15 measured at T = 1.8 K. The sharp kinks mark the lower critical field at ~600 Oe. The orientation of the field with respect to the nanowires was arbitrary.

nanowires *via* the Josephson effect.[25,26] The inset Figure 2b shows an enlarged transition onset. A tiny but sharp downturn in the ZFC magnetization at 11 K can be resolved. This suggests that the nanostructure induces weak diamagnetic fluctuations, 3−4 K above the bulk T_c. The bulk T_c is preceded by a tiny upturn of the magnetization upon decreasing the temperature. Its origin is unclear, but it may be caused by a change in the effective dimensionality when entering the fluctuation regime above the bulk T_c. This may lead to a specific change of the distribution of microscopic screening currents in the entire volume. The much smaller contribution of this fluctuation signal obviously suggests a 1D nature of superconductivity without

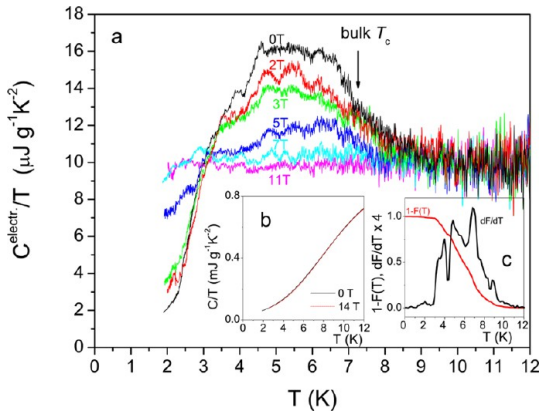

Figure 3. Specific-heat data of Pb-SBA-15. (a) The electronic specific heat in 0, 2, 3, 5, 7, and 11 T shows the broad superconducting transition of Pb-SBA-15 with fluctuations extending up to ~10 K. (b) Total specific heat of Pb-SBA-15 in 0 and 14 T applied magnetic fields (superimposed on this scale). (c) Temperature dependence of the superconducting fraction $1 - F(T)$ in our sample from direct deconvolution of the specific heat[28,33] and the corresponding T_c distribution dF/dT. The orientation of the field with respect to the nanowires was arbitrary.

macroscopic screening currents in this temperature range. Note that the magnetization is relatively insensitive to phase-incoherent superconducting correlations and fluctuation effects, as macroscopic phase coherence is required for the formation of Meissner screening currents. The smallness of this contribution therefore does not necessarily mean that it comes from only a negligible volume fraction of the material. As we will prove later, the specific heat indicates that this contribution is from a significant volume fraction of the sample.

In the inset Figure 2c a magnetization hysteresis loop (recorded at T = 1.8 K) is plotted. It shows the typical behavior of a type-II superconductor. Sharp kinks at ~600 Oe mark the lower critical field (H_{c1}) transition. Above H_{c2}, the amplitude decreases rapidly, but the diamagnetic signal extrapolates toward much higher fields, outside the field range of our magnetometer. Note that bulk Pb is a type-I superconductor. The nanostructuring seems therefore to change the material in a type-II superconductor.

Specific Heat. The inset Figure 3b shows the total specific heat (C/T) of Pb-SBA-15 in 0 and 14 T. Only a tiny difference of 2.6% of the total specific heat (at 5.5 K) can be resolved between the two data sets. Using the 14 T data as approximated normal state background, we analyze the specific heat in a standard way: $C_n(T \rightarrow 0) = \gamma_n T + \sum_{k=1}^{3} \beta_{2k+1} T^{2k+1}$. The first term is the electronic contribution with the Sommerfeld constant γ_n = 10 μJ/gK^2, which comes only from the Pb nanowires. The second term is the low-temperature expansion of the lattice specific heat of Pb and SBA-15 according to the Debye model. Figure 3a shows the electronic contribution C^{electr}/T in various magnetic fields. The 0 T data form the typical broad transition anomaly of a quasi-1D superconductor.[28−32] A sharper jump occurs below 7 K (marked by the arrow), which is certainly related to the main drop of the magnetization. This partial contribution is no longer observed in 2 T, but at least 11 T is necessary to suppress the broad main anomaly, which extends at least to 9−10 K. This confirms that superconducting correlations exist far above the bulk T_c of Pb. This presumably 1D fluctuating contribution (for which the specific heat as a true bulk thermodynamic method is far more sensitive than the magnetization) is surprisingly robust in high magnetic fields, given that the critical field of bulk Pb is only 800 Oe.

For a standard BCS superconductor it is expected that the normalized specific-heat jump at T_c satisfies the relationship $\Delta(C/T_c)/\gamma_n$ = 1.43. This is not evident from our data, as the broad specific-heat jump in C/T (~6 μJ/gK^2) is smaller than γ_n. This discrepancy is due to the broadness of the transition. The high-temperature tail of the specific-heat transition likely originates from the surface layer of the nanowires, which may have a higher T_c. This would create a broad T_c distribution in such thin nanowires, and the BCS relation should be tested separately for each contribution with different T_c. Applying a magnetic field has only a minor effect on the onset temperature of superconductivity, but reduces the overall size of the anomaly. This is surely a consequence of the quasi-1D nature of the material. The T_c distribution can be extracted from the specific heat.[28,33] In Figure 3c, $1 - F(T)$ (temperature dependence of the superconducting fraction in the sample) and dF/dT (T_c distribution) are presented. In dF/dT, a small peak appears (with maximum at 6.9 K and onset at 7.2 K), superimposed on a broad bump, which extends from 3 to 11 K. We attribute the part of the curve above 7.2 K to the surface contribution. The 7.2 K peak may be explained by the onset of 1D superconductivity in the center of the nanowires, while the broad bump represents the crossover from 1D to a 3D bulk superconducting state within the array (as indicated by the appearance of macroscopic screening currents in the magnetization).

Electric Transport. Having probed the bulk superconductivity in Pb-SBA-15 by two complementary thermodynamic methods, we will in the following investigate the electrical transport properties. In Figure 4a the resistance is plotted as measured by a standard four-probe method. A gradual decrease in resistance occurs in zero field, which begins at first sight in the vicinity of the critical temperature of bulk Pb. The resistance approaches zero at ~2 K. Magnetic fields suppress the transition until the normal state is restored in fields slightly higher than 15 T. This high upper critical field is further confirmed by the magnetoresistance data in the inset Figure 4b, which extrapolate to a field-independent value in fields slightly higher than 15 T.

The 15 T data set is free of sharp anomalies in the temperature range between 7 and 20 K and can therefore serve as an approximation of the normal state

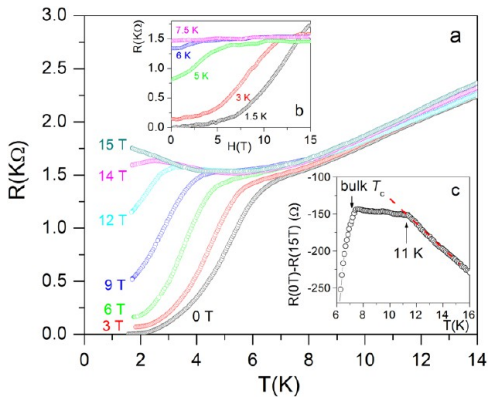

Figure 4. (a) Electrical resistance of Pb-SBA-15. The main figure shows the temperature dependence of the electrical resistance in various magnetic fields in the vicinity of the superconducting transition. (b) Magnetoresistance at various temperatures. (c) Enlarged view of the onset of the transition in zero field after subtraction of 15 T data. The data show that superconducting fluctuations occur up to ~11 K, while the main transition initiates at 7.3 K. The orientation of the field with respect to the nanowires was arbitrary.

background. The inset Figure 4c shows an enlargement of the zero-field transition onset after subtraction of a smooth polynomial fit to the 15 T data. A deviation from the linear temperature dependence at higher temperatures occurs in the form of a sharp drop at ~11 K, which was reproducibly observed in two different devices (see Supporting Information). If we take into account the different sensitivities of our experimental techniques for fluctuating superconductivity, this is consistent with the magnetization and the specific heat. Resistivity thus provides a further indication that superconducting fluctuations extend up to 3−4 K above the bulk T_c. The magnetoresistance data show that superconductivity persists to at least 15 T. The upper critical field (H_{c2} ~15 T) is therefore almost 200 times increased compared to bulk Pb (800 Oe). This change is quite enormous and certainly linked to the dimensionality of the nanowires.

Discussion. Pb-SBA-15, a new form of ultrathin metal nanowire arrays prepared in porous SBA-15 silica matrixes, enables us to study quasi-1D superconductivity in a material, which is in the bulk form a well-known elemental superconductor. The superconducting transition in such arrays of coupled nanowires is quite complex: it is governed by the interplay of strong fluctuations, crossovers in the effective dimensionality, and Josephson coupling. Our data indicate the presence of 1D superconducting correlations at temperatures as high as 10−11 K (3−4 K above the bulk T_c). At lower temperatures, the superconductivity goes through a dimensional crossover to a 3D bulk superconducting state with a clear manifestation of a macroscopic Meissner effect below ~7 K and zero resistance below ~2 K.

Obviously Pb-SBA-15 shows all the characteristics of a type-II superconductor, although Pb in bulk form is a type-I superconductor. Does this imply a change in the material properties in the nanowires? Whether a superconductor is of type-I or type-II depends on the ratio of the penetration depth λ and the coherence length ξ. If Pb-SBA-15 is of type-II, this means that λ/ξ is increased to a value greater than $1/\sqrt{2}$. A change in ξ would mean that the electronic band structure is modified in the individual nanowires. However, Pb is a very good conductor with a high density of charge carriers, and in dimensions of 5 nm, it is unlikely that the bandstructure and hence ξ would change significantly. The penetration depth λ, on the other hand, depends on the charge carrier density, which determines the ability to shield the magnetic field. The carrier density within the individual nanowires should be largely identical to the bulk Pb. However, as we have a composite material made of insulating SBA-15 and superconducting Pb, λ should rather be defined as a characteristic quantity of the entire composite material. For Pb-SBA-15, the carrier density is relatively low, because only a certain volume fraction is occupied by Pb. This means the ability to generate macroscopic Meissner currents is reduced, and this should cause an increase in λ, which is certainly enough to change the composite material in a type-II superconductor.

If the material properties of Pb in the form of ~5 nm thin nanowires remain mostly unchanged, then the high transition onset is rather surprising. The most plausible explanation can be found in the aspect ratio of the ultrathin nanowires. In such thin wires the surface represents a significant fraction of the total volume, and phonon softening[1,34] can cause a locally higher T_c. The surface layer contribution thus becomes observable with bulk thermodynamic methods. T_c enhancements in nanomaterial were previously observed,[3−5,35] but in our material the effect is particularly strong.

The observed increase of the upper critical field from 800 Oe in bulk Pb by a factor of nearly 200 to at least 15 T in arrays of 6 nm thin parallel Pb nanowires is certainly related to their 1D nature. Note that the superconducting composite material Pb-SBA-15 represents an intermediate case between 1D and 3D, as some macroscopic screening currents can be established over the transverse Josephson effect. This is evident, as individual superconducting Pb nanowires of only ~5 nm diameters would fall in any case in the 1D limit, while Pb-SBA-15 shows a Meissner effect, zero resistance, and a well-defined H_{c1} transition.

The standard mechanism of the upper critical field in a type-II superconductor is the "orbital limit" for superconductivity.[36] At this field the vortex cores overlap and the material becomes a normal metal. The formation of vortices requires that Cooper pairs can move on a closed orbit. However, in our nanowire arrays macroscopic screening currents around vortices have to tunnel through the gaps between the wires. This weakens the diamagnetic shielding and pushes the orbital limit to very high field values. The upper

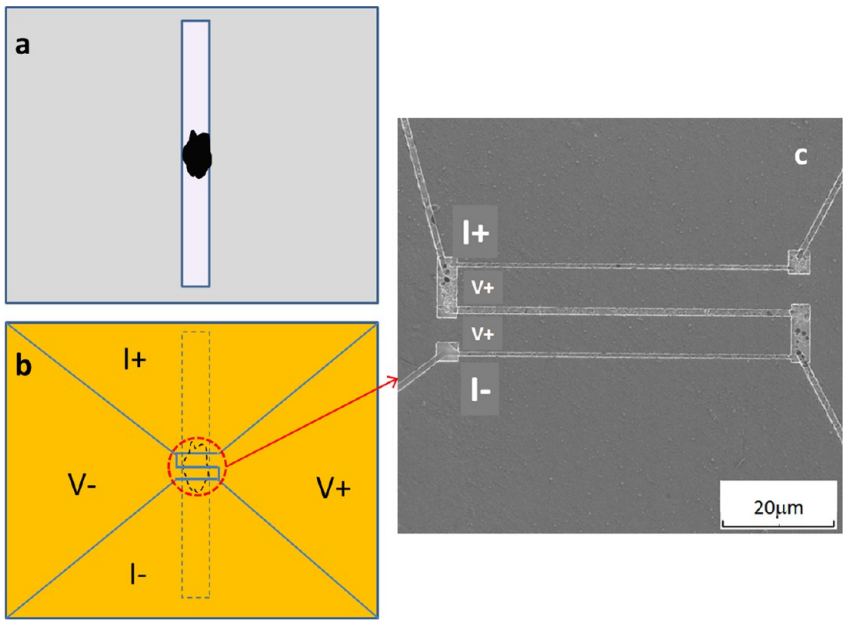

Figure 5. Illustration of the preparation of four-pobe devices for the resistance measurements of Pb-SBA-15. (a) A polycrystalline grain of Pb-SBA-15 is glued into a groove on a silicon substrate. (b) The surface is polished and then covered with a Ti and Au layer. A focused-ion beam technique is used to separate four electrodes (gray lines). (c) SEM image of the center area of the device The separation of the inner voltage terminals (V+ and V−) is 1 μm, while the distance of the outer current terminals (I+ and I−) is 20 μm (see text for details).

critical field can be determined in this case rather by the Pauli limit. In this second characteristic field (which is rarely achieved in conventional bulk superconductors) the Zeeman splitting energy of the two electronic states in the Cooper pair overcomes the binding energy.[37] The Pauli limit should occur at 1.84 T_c (slightly above 13 T) and may be somewhat further enhanced by strong spin−orbit coupling or the formation of a Fulde−Ferrell−Larkin−Ovchinnikov state.[38,39] This is in good agreement with our observation that H_{c2} is slightly higher than 15 T. The replacement of the orbital limit for superconductivity by the Pauli limit thus serves as a likely explanation for the large increase of the upper critical field.

It had been found for individual thicker Pb nanowires that the material of the electrodes can have a strong influence on the superconducting state,[9] even at distances between the voltage terminals exceeding the superconducting coherence length. Could this play a role in the resistance measurement on Pb-SBA-15? This seems not to be the case, since the data from our three experimental probes nicely match each other (note that in the magnetization and specific-heat experiments, there were no electrodes). Indeed Pb-SBA-15 cannot be compared with individual nanowires, as it represents a regular 3D array of nanowires that are weakly coupled through the transverse Josephson effect. Pb-SBA-15 behaves more like a strongly anisotropic bulk superconductor, similar to intrinsically quasi-1D superconductors such as $Tl_2Mo_6Se_6$[29] or $(TMTSF)_2ClO_4$[40] with parallel metallic chains within their crystalline structure. The thickness of our material in the direction perpendicular to the current is a few tens of μm and exceeds the coherence length by 2 orders of magnitude. Therefore, the impact of the electrodes may be hardly observed.

CONCLUSIONS

We have reported a detailed study of the thermodynamic (dc magnetization and specific heat) and electrical transport properties (resistivity) of Pb nanowire arrays in 6 nm pores of mesoporous SBA-15 silica crystal matrixes. An enhancement of the onset of the superconducting transition in the form of fluctuations of up to 3−4 K above the T_c of bulk Pb and an extremely high upper critical field of more than 15 T (almost 200 times higher than the bulk value) were observed and attributed respectively to the significant contribution of surface superconductivity in ultrathin nanowires and the replacement of the orbital limit for superconductivity by the Pauli limit in this quasi-1D superconducting composite material on the nanoscale.

EXPERIMENTAL SECTION

SBA-15 is mesoporous silica and has pores with tunable diameter between 5 and 15 nm.[41] For the growth of the Pb nanowires in the 6 nm pores of SBA-15, a chemical vapor deposition (CVD) technique has been used as described in detail in ref 42. The system consists of a tube furnace, a tubular

CVD reactor with a vacuum pump, and gas sources. For the CVD process, the substrate (SBA-15) was mixed with the precursor (Pb(II) acetylacetonate) and placed in the reactor. The furnace is used to maintain a desired temperature (500 °C) for the deposition to take place. Hydrogen acted as both a reactant and carrier gas and was introduced at a flow rate of 1 sccm during the precursor deposition for chemically reducing the precursor to form elemental lead. In this way, continuous Pb nanowires were formed in the pores of SBA-15, as evidenced by TEM and energy-dispersive X-ray spectroscopy (EDX). High-resolution TEM images showed no significant evidence of a Pb cover layer on the surface of the SBA-15 under these growth conditions. A few Pb nanograins were observed sticking on the surface. However, before the measurements the samples were stored for several weeks in a dry cabinet. At the time of the measurement we verified by TEM that all such Pb clusters were fully oxidized and insulating, while the nanowires in the pores were protected and kept their metallic character. The length of the nanowires is determined mainly by the size of the SBA-15 crystals, which were long columns, a few hundred nm thick, and with a length of 500 nm to a few μm. The average center–center spacing between the nanowires is 9 nm.

The magnetization was measured with a commercial Quantum Design Vibrating-Sample SQUID magnetometer under ZFC and FC conditions and in field sweeps at fixed temperatures. The small, mostly temperature-independent linear diamagnetic contribution of SBA-15 was determined separately and subtracted from the data. For the temperature-sweep data taken in a field of only 5 Oe it disappeared into the noise.

A homemade microcalorimeter was used for the specific-heat measurements. A standard ac technique[43] was used, which provides high relative resolutions ($\Delta C/C$) of 10^{-4} to 10^{-5}. The thermometry was calibrated very precisely in magnetic fields up to 14 T. To remove the dominant phonon background of SBA-15, the 14 T data were subtracted as a background, unless otherwise indicated.

The electrical resistivity was measured with a Keithley model 6221 ac current source in combination with a Stanford Research 830 digital lock-in amplifier. A polycrystalline grain was glued with epoxy resin in a groove, which has previously been cut by a laser into a Si substrate. The grain was then polished, and 15 nm of Ti was sputtered on the surface followed by 135 nm of Au. Four electrodes were separated by a focused ion beam technique. Figure 5 shows an illustration of the fabrication process with a scanning electron microscope (SEM) image of the electrical contacts. The distance between the voltage terminals was 1 μm, and the distance between the current contacts was 20 μm. The orientation of the nanowires in relation to the current was arbitrary. A standard four-probe technique was used. Because of the small size and difficulties in accurate assessment of the current path in the device, we present the resistance rather than the resistivity.

Although the local filling factor of the silica pores can reach high values close to 100% over length scales of a few 100 nm (as evidenced by TEM in Figure 1), such Pb-rich regions were typically separated by Pb-poor areas along the grain boundaries. Therefore, the exact Pb content of the material was unknown, and we did not attempt to extract information about the absolute values of our thermodynamic probes. Instead, we normalized the data per gram of this composite material instead of per mole. Note that in all the measurements the magnetic field direction relative to the nanowires was arbitrary. This is a consequence of the polycrystalline nature of the material.

Conflict of Interest: The authors declare no competing financial interest.

Acknowledgment. We thank U. Lampe for technical support and K. Law, M. Cohen, S. Louie for stimulating discussions. This work was supported by the Research Grants Council of Hong Kong, Grant Nos. SEG-HKUST03 and 603010.

Supporting Information Available: Resistance data from a second device. This material is available free of charge *via* the Internet at http://pubs.acs.org.

REFERENCES AND NOTES

1. Watson, J. H. P. Transition Temperature of Superconducting Indium, Thallium, and Lead Grains. *Phys. Rev. B* **1970**, *2*, 1282–1286.
2. Li, W.-H.; Yang, C. C.; Tsao, F. C.; Wu, S. Y.; Huang, P. J.; Chung, M. K.; Yao, Y. D. Enhancement of Superconductivity by the Small Size Effect in In Nanoparticles. *Phys. Rev. B* **2005**, *72*, 214516–214520.
3. Charnaya, E. V.; Tien, C.; Lin, K. J.; Wur, C. S.; Kumerzov, Yu. A. Superconductivity of Gallium in Various Confined Geometries. *Phys. Rev. B* **1998**, *58*, 467–472.
4. Hagel, J.; Kelemen, M. T.; Fischer, G.; Pilawa, B.; Wosnitza, J.; Dormann, E.; Löhneysen, H. v.; A Schnepf, A.; Schnöckel, H.; Neisel, U.; *et al.* Superconductivity of a Crystalline Ga_{84}-Cluster Compound. *J. Low Temp. Phys.* **2002**, *129*, 133–142.
5. Ohshima, K.; Fujita, T. Enhanced Superconductivity in Layers of Ga Fine Particles. *J. Phys. Soc. Jpn.* **1986**, *55*, 2798–2802.
6. Wang, J.; Ma, X.; Ji, S.; Qi, Y.; Fu, Y.; Jin, A.; Lu, L.; Gu, C.; Xie, X. C.; Tian, M.; *et al.* Magnetoresistance Oscillations of Ultrathin Pb Bridges. *Nano Res.* **2009**, *2*, 671–677.
7. Wang, J.; Ma, X. C.; Lu, L.; Jin, A. Z.; Gu, C. Z.; Xie, X. C.; Jia, J. F.; Chen, X.; Xue, Q. K. Anomalous Magnetoresistance Oscillations and Enhanced Superconductivity in Single-Crystal Pb Nanobelts. *Appl. Phys. Lett.* **2008**, *92*, 233119.
8. Hsu, Y.-J.; Lu, S.-Y.; Lin, Y.-F. Nanostructures of Sn and Their Enhanced, Shape-Dependent Superconducting Properties. *Small* **2006**, *2*, 268–273.
9. Wang, J.; Sun, Y.; Tian, M.; Liu, B.; Singh, M.; Chan, M. H. W. Superconductivity in Single Crystalline Pb Nanowires Contacted by Normal Metal Electrodes. *Phys. Rev. B* **2012**, *86*, 035439.
10. Xu, K.; Heath, K. Controlled Fabrication and Electrical Properties of Long Quasi-One-Dimensional Superconducting Nanowire Arrays. *Nano Lett.* **2008**, *8*, 136–141.
11. Tian, M.; Wang, J.; Kurtz, J. S.; Liu, Y.; Chan, M. H. W.; Mayer, T. S.; Mallouk, T. E. Dissipation in Quasi-One-Dimensional Superconducting Single-Crystal Sn Nanowires. *Phys. Rev. B* **2005**, *71*, 104521–104527.
12. Van Hove, L. The Occurrence of Singularities in the Elastic Frequency Distribution of a Crystal. *Phys. Rev.* **1953**, *89*, 1189–1193.
13. Hohenberg, P. C. Existence of Long Range Order in One and Two Dimensions. *Phys. Rev.* **1967**, *158*, 383–386.
14. Mermin, N. D.; Wagner, H. Absence of Ferromagnetism or Antiferromagnetism in One- or Two-Dimensional Isotropic Heisenberg Models. *Phys. Rev. Lett.* **1966**, *17*, 1133–1136.
15. Langer, J. S.; Ambegaokar, V. Intrinsic Resistive Transition in Narrow Superconducting Channels. *Phys. Rev.* **1967**, *164*, 498–510.
16. McCumber, D. E.; Halperin, B. I. Time Scale of Intrinsic Resistive Fluctuations in Thin Superconducting Wires. *Phys. Rev. B* **1970**, *1*, 1054–1070.
17. Stoeckly, B.; Scalapino, D. J. Statistical Mechanics of Ginzburg-Landau Fields for Weakly Coupled Chains. *Phys. Rev. B* **1975**, *11*, 205–210.
18. Scalapino, D. J.; Imry, Y.; Pincus, P. Generalized Ginzburg-Landau Theory of Pseudo-One-Dimensional Systems. *Phys. Rev. B* **1975**, *11*, 2042–2048.
19. Kobayashi, K.; Stroud, D. Theory of Fluctuations in a Network of Parallel Superconducting Wires. *Phys. C* **2011**, *471*, 270–276.
20. Schulz, H. J.; Bourbonnais, C. Quantum Fluctuations in Quasi-One-Dimensional Superconductors. *Phys. Rev. B* **1983**, *27*, 5856–5859.
21. Gorkov, L. P.; Dzyaloshinskii, I. E. Possible Phase Transitions in Systems of Interacting Metallic Filaments (Quasiunidimensional Metals). *Zh. Eksp. Teor. Fiz.* **1974**, *67*, 397–417.
22. Klemm, R. A.; Gutfreund, H. Order in Metallic Chains. II. Coupled Chains. *Phys. Rev. B* **1976**, *14*, 1086–1102.
23. Lee, P. A.; Rice, T. M.; Klemm, R. A. Role of Interchain Coupling in Linear Conductors. *Phys. Rev. B* **1977**, *15*, 2984–3002.
24. Efetov, K. B.; Larkin, A. I. Effect of Fluctuations on the Transition Temperature in Quasi-One Dimensional Superconductors. *Sov. Phys. JETP* **1975**, *41*, 76–79.

25. Bergk, B.; Petrović, A. P.; Wang, Z.; Wang, Y.; Salloum, D.; Gougeon, P.; Potel, M.; Lortz, R. Superconducting Transitions of Intrinsic Arrays of Weakly Coupled One-Dimensional Superconducting Chains: The Case of the Extreme Quasi-1D Superconductor $Tl_2Mo_6Se_6$. *New J. Phys.* **2011**, *13*, 103018.
26. Wang, Z.; Shi, W.; Xie, H.; Zhang, T.; Wang, N.; Tang, Z. K.; Zhang, X. X.; Lortz, R.; Sheng, P.; Sheikin, I.; *et al*. Superconducting Resistive Transition in Coupled Arrays of 4 Å Carbon Nanotubes. *Phys. Rev. B* **2010**, *81*, 174530–174539.
27. Michotte, S.; Piraux, L.; Dubois, S.; Pailloux, F.; Stenuit, G.; Govaerts, J. Superconducting Properties of Lead Nanowires Arrays. *Phys. C (Amsterdam, Neth.)* **2002**, *377*, 267–276.
28. Shi, W.; Wang, Z.; Zhang, Q.; Zheng, Y.; Ieong, C.; He, M.; Lortz, R.; Cai, Y.; Wang, N.; Zhang, T.; *et al*. Superconductivity in Bundles of Double-Wall Carbon Nanotubes. *Sci. Rep.* **2012**, *2*, 625.
29. Petrović, A. P.; Lortz, R.; Santi, G.; Decroux, M.; Monnard, H.; Boeri, L.; Andersen, O. K.; Kortus, J.; Salloum, D.; Gougeon, P.; *et al*. Phonon Mode Spectroscopy, Electron-Phonon Coupling and the Metal-Insulator Transition in Quasi-One-Dimensional $M_2Mo_6Se_6$. *Phys. Rev. B* **2010**, *82*, 235128–235143.
30. Lortz, R.; Zhang, Q.; Shi, W.; Ye, J.; Qiu, C.; Wang, Z.; He, H.; Sheng, P.; Qian, T.; Tang, Z. K.; *et al*. Superconducting Characteristics of 4-Å Carbon Nanotube-Zeolite Composite. *Proc. Natl. Acad. Sci. U.S.A.* **2009**, *106*, 7299–7303.
31. Wang, Z.; Shi, W.; Lortz, R.; Sheng, P. Superconductivity in 4-Angstrom Carbon Nanotube Arrays—A Short Review. *Nanoscale* **2012**, *4*, 21–41.
32. Scheidt, E.-W.; Hauf, C.; Reiner, F.; Eickerling, G.; Scherer, W. Possible Indicators for Low Dimensional Superconductivity in the Quasi-1D Carbide Sc_3CoC_4. *J. Phys. Conf. Ser.* **2011**, *273*, 012083–012086.
33. Wang, Y.; Senatore, C.; Abächerli, V.; Uglietti, D.; Flükiger, R. Specific Heat of Nb_3Sn Wires. *Supercond. Sci. Technol.* **2006**, *19*, 263–266.
34. Kresin, V. Z.; Ovchinnikov, Yu N. `Giant' Strengthening of Superconducting Pairing in Metallic Nanoclusters: Large Enhancement of T_c and Potential for Room-Temperature Superconductivity. *Sov. Phys. Usp.* **2008**, *51*, 427–435.
35. Cohen, R. W.; Abeles, B. Superconductivity in Granular Aluminum Films. *Phys. Rev.* **1968**, *168*, 444–450.
36. Gor'kov, L. P. The Critical Supercooling Field in Superconductivity Theory. *Sov. Phys. JETP* **1960**, *10*, 593–599.
37. Chandrasekhar, B. S. A Note on the Maximum Critical Field of High-Field Superconductors. *Appl. Phys. Lett.* **1962**, *1*, 7–8.
38. Fulde, P.; Ferrell, R. A. Superconductivity in a Strong Spin-Exchange Field. *Phys. Rev.* **1964**, *135*, A550–A563.
39. Larkin, A. I.; Ovchinnikov, Y. N. Quasiclassical Method in the Theory of Superconductivity. *Sov. Phys. JETP* **1965**, *20*, 762–769.
40. Bourbonnais, C.; Jérome, D. Interacting Electrons In Quasi-One-Dimensional Organic Superconductors, In *The Physics of Organic Superconductors and Conductors*; Lebed, A., Eds.; Springer Series in Materials Science Vol. 110, Springer: Heidelberg, 2008; pp 357—414.
41. Zhao, D. Y.; Feng, J. L.; Huo, Q. S.; Melosh, N.; Fredrickson, G. H.; Chmelka, B. F.; Stucky, G. D. Triblock Copolymer Syntheses of Mesoporous Silica with Periodic 50 to 300 Angstrom Pores. *Science* **1998**, *279*, 548–552.
42. Zhang, Y.; Lam, F. L. Y; Hu, X.; Yan, Z. F.; Sheng, P. Fabrication of Copper Nanowire Encapsulated in the Pore Channels of SBA-15 by Metal Organic Chemical Vapor Deposition. *J. Phys. Chem. C* **2007**, *111*, 12536–12541.
43. Sullivan, P. F.; Seidel, G. Steady-State, AC-Temperature Calorimetry. *Phys. Rev.* **1968**, *17*, 679–685.